

# An Automated 3D Segmented and DWT Enhanced Model for Brain MRI

B. Naresh Kumar, Dr.M.Sailaja M.S (U.S.A), Ph.D

**Abstract-** This correspondence deals with the development of an automated 3-D segmentation and DWT enhanced model for Brain MRI. The proposal model of segmentation is a model-based approach for accurate, robust, and automated tissue segmentation of brain MRI data of single as well as multiple magnetic resonance sequences. The main contribution of this study is that we employ an edge-based geodesic active Contour for the segmentation task by integrating both image edge geometry and voxel statistical homogeneity into a novel hybrid geometric-statistical feature to regularize contour convergence and extract complex anatomical structures. We validate the accuracy of the segmentation results on simulated brain MRI scans of single T1-weighted and multiple T1/ T2/PD weighted sequences. When compared to a current state-of-the-art region based level-set segmentation formulation, our white matter and gray matter segmentation resulted in significantly higher accuracy levels with a mean improvement in Dice similarity indexes and The proposed resolution enhancement technique uses DWT to decompose the input image into different sub bands. Then, the high-frequency sub band images and the input low-resolution image have been interpolated, followed by combining all these images to generate a new resolution-enhanced image by using inverse DWT. In order to achieve a sharper image, an intermediate stage for estimating the high-frequency sub bands has been proposed. The proposed technique has been tested on brain MRI images. The quantitative (peak signal-to-noise ratio and root mean square error) and visual results show the superiority of the proposed technique over the conventional and state-of-art image resolution enhancement techniques. Thus the development of the project is done using MATLAB simulation for results.

**Keywords:**

3-D segmentation, deformable models, brain segmentations. Discrete wavelet transform (DWT), interpolation, Brain MRI image resolution enhancement, wavelet zero padding (WZP).

## 1. INTRODUCTION

MRI Stands for Magnetic Resonance Imaging; once called Nuclear Magnetic Resonance Imaging. The "Nuclear" was dropped off about 15 years ago because of fears that people would think there was something radioactive involved, which there is not. MRI is a way of getting pictures of various parts of your body without the use of x-rays, unlike regular x-rays pictures and CAT scans. A MRI scanner consists of a large and very strong magnet in which the patient lies. A radio wave antenna is used to send signals\* to the body and then receive signals back. These returning signals are converted into pictures by a computer attached to the scanner. Pictures of almost any part of your body can be obtained at almost any particular angle. These "radio wave signals" are actually a varying or changing magnetic field that is much weaker than the steady, strong magnetic field of the main magnet. Resolution of an image has been always an important in many image- and video-processing applications, such as video resolution issue enhancement, feature extraction and image resolution enhancement. Interpolation has been widely used in many image processing applications, such as facial reconstruction, multiple description coding, and image resolution enhancement. The interpolation-based image resolution enhancement has been used for a long time and many interpolation techniques have been developed to increase the quality of this task. There are three well-known interpolation techniques, namely, nearest neighbor, bilinear, and bicubic. Bicubic interpolation is more sophisticated than the other two techniques and produces smoother edges. the proposed wavelet based resolution enhancement Technique.

### A. Safety in MRI

MRI is quite safe in the majority of patients. Certain patients may not be able to have an MRI. These include people who get nervous in small spaces (claustrophobic) and those with implanted medical devices such as aneurysm clips in the brain, heart pacemakers and cochlear (inner ear) implants. Also, people with pieces of metal close to or in an important organ (such as the eye) may not be scanned. There are a few additional safety considerations and some exceptions based on individual circumstances. Also, certain metal objects that we common have on our persons like watches, credit cards, hair pins, writing pens, etc. may be damaged by the MRI scanner or may be pulled away from our bodies if we go into an MRI room. Also, metal can sometimes cause poor pictures if it is close to the part being scanned. For these reasons, patients are asked to remove these objects before entering the MRI scanner.

### B.MRI Examination

You will most likely be lying on a special table that moves into the centre of the magnet. Prior to going into the magnet you will be offered earplugs to reduce the noise that you hear. You will then hear some "hammering" noises while the scanner is preparing for scanning and taking the pictures. During this hammering noise, it is important not to move, as this would blur the pictures. You may also feel some vibration during the hammering noise and some slight movement of the table during the examination. Some patients will be given an injection in their arm of a substance that improves certain types of pictures.

This substance, called a "contrast agent", is very safe and is unrelated to the iodine used for CAT scans and kidney x-rays.

### C. Advantages of a MRI scan

- MRI scanners are good at looking at the non-bony parts or "soft tissues" of the body. In particular, the brain, spinal cord and nerves are seen much more clearly with MRI than with regular x-rays and CAT scans.
- Also, muscles, ligaments and tendons are seen quite well so that MRI scans are commonly used to look at knees and shoulders following injuries.
- A MRI scanner uses no x-rays or other radiation.
- A disadvantage of MRI is its higher cost compared to a regular x-ray or CAT scan. Also, CAT scans are frequently better at looking at the bones than MRI.

## II. PROPOSED SYSTEM (SEGMENTATION)

### A. Edge based deformable model:

We utilize the geodesic active contour model rather than the region-based formulation due to its computation soundness and extendibility. The geodesic model delineates region boundaries by describing the evolution of a curve or surface C from an initial position C0 as finding the minima of the Riemannian curve distance

$$\min \int_0^1 g(|\nabla I(C(q))|) |C'(q)| dq$$

$$= \min \int_0^{L(C)} g(|\nabla I(C(s))|) ds \quad \dots\dots\dots 1$$

Where g is a general feature function, |∇I| is the gradient norm of intensity I, and q is the parameterization of the curve C. The right side of the equation describes the parameterized curve C(q) such that the Euclidean length of C can be represented as L(C) = ∫₀¹ |C'(q)| dq = ∫₀¹ ds, where ds = |C'(q)| dq is the Euclidean arc length or the Euclidean metric. Note that this geodesic formulation of the active contour relies on g, the speed and halting feature for the evolving surface in 3-D applications derived based on the geometric gradient feature of an image. Generally, g is chosen as a positive-valued function of the intensity gradient as in (1), where I is a smoothed version of I and q = 1 or 2. Other similar monotonically decreasing functions, such as the sigmoid function (2) with parameters α (width of intensity window) and β (centre of intensity window) are also often utilized. The value of this feature function determines the propagation of the surface by searching for the minimal Riemannian distance is equation (2). An ideal edge would ultimately have a feature value of zero at all the pixel points along this boundary. However, propagation relying

solely on edge feature is typically sensitive to noisy and weak edges that are frequently observed in medical images.

$$g = \left( 1 + \exp \left[ \frac{|\nabla I| - \beta}{\alpha} \right] \right)^{-1} \quad \dots\dots\dots 2$$

In particular, with the presence of complex anatomical structures, it is often impossible to automatically and accurately derive the desired geometric edge term to prevent contour leakage into the surrounding regions. Consequently, achieving accurate segmentation results with edge-based geodesic active contour requires either user intervention or careful adjustment of parameters such that the ideal boundary is minimal. This process is subjective and ideal parameters are often difficult to derive for a fully automated segmentation framework.

### B. Hybrid geometric-statistical feature

We propose to transform the feature function g in the traditional geodesic active contour formulation into a hybrid feature function by incorporating geometric image features with voxel statistics to help automate and regularize the evolving contours. The minimization of the active contour is thus represented by

$$\min \int_0^{L(C)} g(|\nabla I(C(s))|) P(I|\Phi) ds \quad \dots\dots\dots 3$$

Where for gray-scale intensity MR images, P(I|Φ) represents the probability distribution function of a mixture model (3) from which voxel statistics are drawn, assuming that all voxels are identically and independently distributed and the image is to be described with K class labels.

$$P(I|\Phi) = \sum_{k=1}^K P(k) P(I|\Phi_k) \quad \dots\dots\dots 4$$

Where P(k) represents the prior probability of the class label k and P(I|Φk) is the conditional density function of the kth class given Φ, the parameter set of the distribution. We employ Gaussian distributions as

$$P(I|\Phi) = \left[ \frac{1}{\sigma \sqrt{2\pi}} \right] \exp \left[ \frac{-(I - \mu)^2}{2\sigma^2} \right] \quad \dots\dots\dots 5$$

Which require a parameter set Φ = {μ, σ}, where μ and σ are the mean and standard deviation. This parameter estimation problem for GMM is solved by applying the EM algorithm to the image intensity histogram. The design of g in (2) utilizes both a geometric term and a statistical term. Geometrically, the presence of strong image gradients indicates significant structural content. As a result, the contour propagation speed slows to a halt. On the other hand, a lack of edge features

often indicates the presence of a homogeneous region. Statistically, high voxel probability indicates a high likelihood of the voxel belonging to the class of interest, warranting a

$$\frac{\partial u}{\partial t} = g(I)(\phi_k + c)|\nabla u| + \varepsilon \nabla g(I) \cdot \nabla u \quad \dots\dots 9$$

fast contour propagation. If the voxel likelihood is reduced, the contour propagation is slowed down accordingly. The contribution of voxel likelihood to the contour propagation exhibits an inverse behavior to that of image gradients. Since both geometric and statistical features are essential to the contour stability, they can be combined into a Single hybrid feature function by modelling the aforementioned Behaviour

$$g(\mathbf{C}) = \text{sigmoid}(|\nabla I|) \text{sigmoid}^{-1}(P(I|\Phi))$$

$$\text{as as} = \left( 1 + \exp \left[ \frac{|\nabla I| - \beta}{\alpha} \right] \right)^{-1} \left[ -\ln \left( \frac{1 - P(I|\Phi)}{P(I|\Phi)} \right) \right]$$

.6

Where the first term is the traditional geometric feature as in (6) and the second term models the inverse behaviour of voxel likelihood to image gradients using an inverse sigmoid function with magnitudes between -1 and 1. Complementarily, these two components in the new hybrid feature help regularize the evolving contour in both the geometric and statistical sense. The minimization of (7) is then achieved by computing the Euler-Lagrange equation

$$\frac{d}{dt} \int_0^1 g(\mathbf{C}(q)) |C'(q)| dq \Big|_{t=0} = \int_0^{L(C_0)} \left( \kappa g(C_0) * \vec{N} \cdot \vec{N} - g(C_0)_k \vec{N} \right) \cdot \vec{C}_0 ds \quad \dots\dots 7$$

Where  $\kappa$  is the Euclidean curvature,  $\vec{N}$  is the inward unit normal, and  $C_0$  is the initial curve or surface, and performing steepest gradient search (8), to deform  $C$  toward a minima

$$\frac{\partial C}{\partial t} = g(I)(\phi_k + c)\vec{N} - \varepsilon \nabla g \cdot \vec{N} \vec{N} \quad C(0) = C_0 \dots\dots 8$$

Where  $\{\psi, c, \varepsilon\}$  are the free parameters introduced to govern curvature, propagation, and advection strengths, respectively. With the designed hybrid feature, the algorithm uses only the propagation term. Other terms are shown here for completeness. This curve evolution equation is then embedded in a level set function  $u$  and solved for the steady state solution

The numerical implementation is based on the curve evolution algorithm via level sets, which utilizes an upwind piecewise continuous approximation scheme to provide a numerically stable solution in the presence of singularities. As summarized in Table (I), the rationale behind using this new hybrid feature is to enable handling of situations where

Table 1:

Effects of Regularizing Contour Propagation using Geometric and Statistical features

		Statistical Feature (probability)	
		Low	High
Geometric Feature (gradient magnitude)	High	↓ Speed Deflation	↓ Speed Inflation
	Low	↑ Speed Deflation	↑ Speed Inflation

The image gradient is high (small sigmoid(|∇I|) value) and The posterior probability of voxel is low, in which the voxel is considered to be a significant feature but lies outside of the desired region. We, therefore, aim to steer the contour slowly away from this voxel by assigning a small negative feature value. On the other hand, if the posterior probability is high, this indicates a significant feature within the desired region; therefore, a small positive feature value is assigned. In contrast, if the image gradient is low (large sigmoid(|∇I|) value) and the posterior probability is low, the voxel is considered to be a weak gradient feature that lies outside of the desired region, warranting a large negative feature value such that contour can be quickly steered away from that region. If the posterior probability is high, a homogeneous area in the desired region is indicated, and is rewarded with a large positive feature value for fast contour expansion. In summary, the proposed hybrid feature provides an adaptive active contour propagation based on local information reflecting both geometry and statistical homogeneity.

C. Segmentation of Brain MRI

Based on the proposed active contour model, we develop a fully automated 3-D brain tissue segmentation algorithm for MRI images. We first present the proposed algorithm for T1-weighted (T1w) MRI scans, which are most often used for brain tissue segmentation due to the generally high WM and GM contrast and the reduced effects of WM Lesions in patients with neurodegenerative diseases. We later extend the proposed method to simultaneously incorporate additional MR sequence data, such as T2-weighted (T2w) and PD-

weighted (PDW) images, in addition to T1w. To segment the brain tissues, we first estimate the GMM parameters such that each mixture distribution represents one single class. Based on these estimated distributions, the normalized posterior probability of each voxel is calculated. We derive the hybrid geometric-statistical feature as described above by combining both the voxel statistics and the image gradient information.

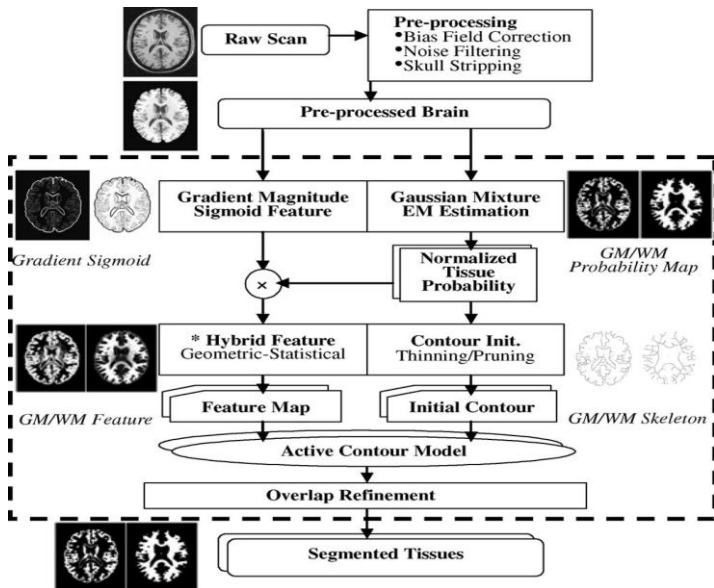


Fig. 1

### III Wavelet-Based Image Resolution Enhancement

There are several methods which have been used for Brain MRI resolution enhancement. In this paper, we have used two state-of-art techniques for comparison purposes. The first one is WZP and CS, and the second one is the previously introduced CWT-based image resolution enhancement

#### A. CS Based Image Resolution Enhancement

This method adopts the CS methodology in the wavelet Domain. The algorithm consists of two main steps as follows:

- 1) An initial approximation to the unknown high resolution image is generated using wavelet domain zero padding (WZP).
- 2) The cycle-spinning methodology is adopted to operate the following tasks:

a) A number of low resolution images are generated from the obtained estimated high resolution image in part (1) by spatial shifting, wavelet transforming, and discarding the high frequency sub bands.

b) The WZP processing is applied to all those low resolution images yielding N high resolution images.

c) These intermediated high resolution images are realigned and averaged to give the final high resolution reconstructed image.

Shows the block diagram of the WZP- and CS-based image super resolution.

#### B.CWT-Based Image Resolution Enhancement

In this technique, dual-tree CWT (DT-CWT) is used to decompose an input image into different sub band images. DT-CWT is used to decompose an input low-resolution image into different sub bands. Then, the high-frequency sub band images and the input image are interpolated, followed by combining all these images to generate a new high-resolution image by using inverse DT-CWT. The resolution enhancement is achieved by using directional selectivity provided by the CWT, where the high-frequency sub bands in six different directions contribute to the sharpness of the high-frequency details, such as edges. Details of this technique are shown in Fig. 2, where the enlargement factor through the resolution enhancement is  $\alpha$ .

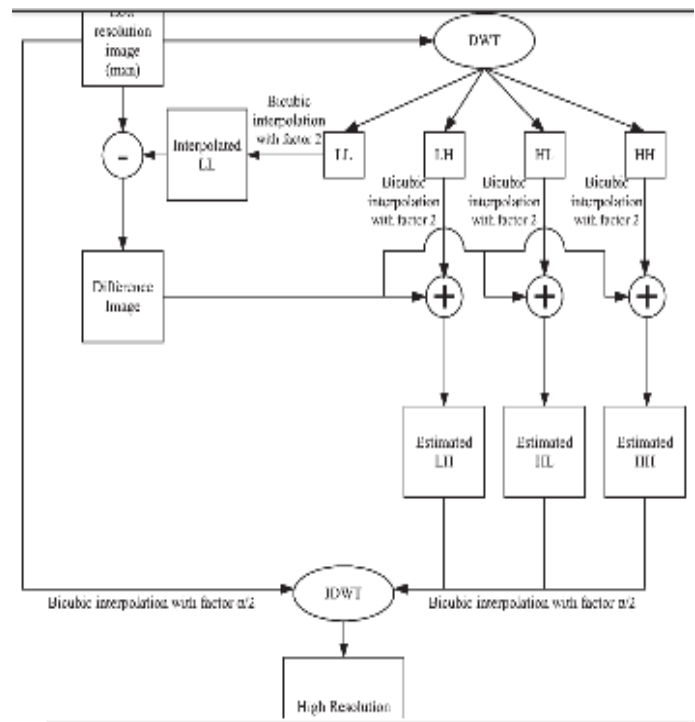


Fig. 2

#### C. Proposed System (DWT-Based Resolution Enhancement)

As it was mentioned before, resolution is an important feature in brain MRI imaging, which makes the resolution enhancement of such images to be of vital importance as increasing the resolution of these images will directly affect the performance of the system using these images as input. The main loss of an image after being resolution enhanced by applying interpolation is on its high-frequency components, which is due to the smoothing caused by interpolation. Hence, in order to increase the quality of the enhanced image, preserving the edges is essential. In this paper, DWT [4] has been employed in order to preserve the high-frequency components of the image. DWT separates the image into different sub band images, namely, LL, LH, HL, and HH. High-frequency sub bands contain the high frequency component of the image. The



interpolation can be applied to these four sub band images. In the wavelet domain, the low-resolution image is obtained by low-pass filtering of the high-resolution image as in [2], [4], and [6]. The lower resolution image (LL sub band), without quantization (i.e., with double-precision pixel values) is used as the input for the proposed resolution enhancement process. Therefore, instead of using low-frequency sub band images, which contains less information than the original input image, we are using this input image through the interpolation process. Hence, the input low-resolution image is interpolated with the half of the interpolation factor,  $\alpha/2$ , used to interpolate the high-frequency sub bands. In order to preserve more edge information, i.e., obtaining a sharper enhanced image, we have proposed an intermediate stage in high frequency sub band interpolation process. The low-resolution input brain MRI image and the interpolated LL image with factor 2 are highly correlated. The difference between the LL sub band image and the low-resolution input image are in their high-frequency components. Hence, this difference image can be use in the intermediate process to correct the estimated high-frequency components. This estimation is performed by interpolating the high-frequency sub bands by factor 2 and then including the difference image (which is high-frequency components on low-resolution input image) into the estimated high-frequency images, followed by another interpolation with factor  $\alpha/2$  in order to reach the required size for IDWT process. The intermediate process of adding the difference image, containing high-frequency components, generates significantly sharper and clearer final image. This sharpness is boosted by the fact that, the interpolation of isolated high-frequency components in HH, HL, and LH will preserve more high-frequency components than interpolating the low-resolution image directly.

**Table 2:**

PSNR results for different methods:

Method \ Image	PSNR (db)	
	Fig 3	Fig 4
Bicubic	19.89	17.23
Bilinear	17.30	18.07
Wavelet zero padding	21.08	18.85
The proposed Method	22.02	24.40

Not only visual comparison but also quantitative comparisons are confirming the superiority of the proposed method. Peak signal-to-noise ratio (PSNR) and root mean square error (RMSE) have been implemented in order to obtain some quantitative results for comparison. PSNR can be obtained by using the following formula:

$$PSNR = 10 \log_{10} \left( \frac{R^2}{MSE} \right) \quad \dots\dots 10$$

Where  $R$  is the maximum fluctuation in the input image are represented by 8 bit, i.e., 8-bit grayscale representation have been used—radiometric resolution is 8 bit); and  $MSE$  is representing the MSE between the given input image  $I_{in}$  and the original image  $I_{org}$  which can be obtained by the following:

$$MSE = \frac{\sum_{i,j} (I_{in}(i,j) - I_{org}(i,j))^2}{M \times N} \quad \dots\dots 11$$

Where  $M$  and  $N$  are the size of the images. Clearly, RMSE is the square root of MSE; hence it can be calculated by the following:

$$RMSE = \sqrt{\frac{\sum_{i,j} (I_{in}(i,j) - I_{org}(i,j))^2}{M \times N}} \quad \dots\dots 12$$

Table (II) is showing the comparison between the proposed method using discrete wavelet transform with bicubic interpolation and some state-of-art resolution enhancement techniques, such as BICUBIC, BILINEAR and WAVELET ZERO PADDING technique, and also the formerly proposed resolution enhancement technique by means of calculating PSNR. In order to show the improvement obtained by the proposed image resolution enhancement from information content point of view, the entropy of Figs. (3) And (4) have been calculated. Table II is showing these entropy values. As expected, highest level of Information content is embedded in the original images. The main reason of having the relatively high information content level of the images generated by the proposed method is due to the fact that the unquantized input LL-sub band images contain most of the information of the original high-resolution image. A possible unsigned 8-bit representation of the LL-sub band image would introduce irreversible quantization loss of information which is given in the first row of Table II. As it was mentioned in the previous section, the low resolution input images are obtained by down sampling the high-resolution images. This approach can be tolerated in some applications where there is no limitation in the number of bits for the representation of floating point numbers. However, in some applications, the down sampled images have to go through a quantization process where the fractions are removed to accommodate 8-bit unsigned integer representation. In order to show the effect of the quantization loss embedded in 8-bit unsigned integer representation, the proposed resolution enhancement technique has been applied to quantized images, and the

results are reported in Tables 2. The results are confirming the expectation of performance drop on the proposed algorithm due to the loss of information contained in the floating points. The intermediate process of adding the difference image, containing high-frequency components, generates significantly sharper and clearer final image. This sharpness is boosted by the fact that, the interpolation of isolated high-frequency components in HH, HL, and LH will preserve more high-frequency components than interpolating the low-resolution image directly.

## RESULTS:

### 1. Result for 3D Segmentation:

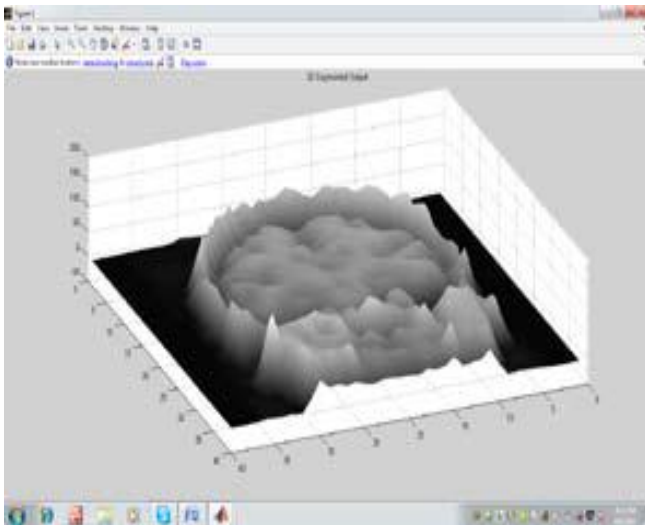


Fig. 3

### 2. Result for DWT Enhanced Model:

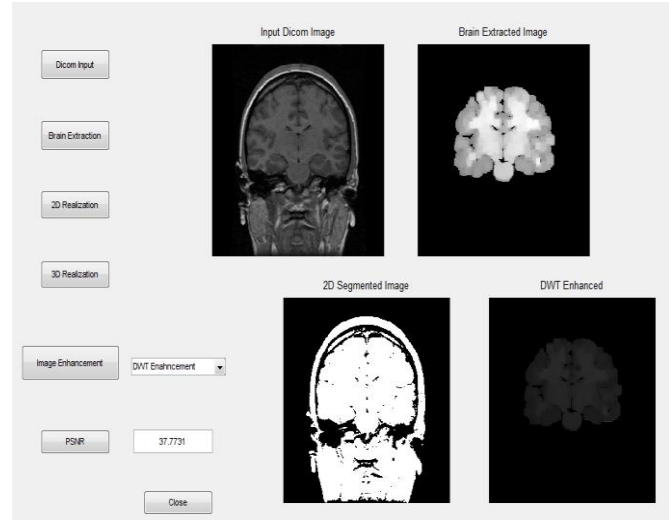


Fig. 4

## Conclusion:

We proposed a 3-D brain MR segmentation method based on deformable models and demonstrated accurate and stable brain tissue segmentation on single as well as multiple MR sequence scans. The main contribution of our work is that we employed a geodesic active contour formulation by integrating both image geometry and voxel statistics into a hybrid geometric–statistical feature; we validated our technique first by using both single and multiple simulated brain MRI sequence data. Improved segmentation accuracy and robustness were shown in results from the proposed hybrid approach against those using individual geometric or statistical features only. Further more, on real clinical MRI datasets, we also demonstrated improved accuracy over a state-of-the-art approach, the region-based M3DLS. Issues identified for possible future work include enhancing the statistical distribution estimation process by using complex intensity distribution estimation methods such as nonparametric and partial volume models, and extending additional segmentation classes, feature cues for segmentation of anomalies such as tumors. The DWT and the input image technique has been tested on well-known benchmark images, where their PSNR and RMSE and visual results show the superiority of the proposed technique over the conventional and state-of-art image resolution enhancement techniques. The PSNR improvement of the proposed technique is up to 7.19 dB compared with the standard bicubic interpolation

## References:

- [1] M. K. Beyer, C. C. Janvin, J. P. Larsen, D. Aarsland, "An MRI study of patients with Parkinson's disease with mild cognitive impairment and dementia using voxel based morphometry," *J. Neurol. Neurosurg. Psychiatry*, vol. 78, no. 3, pp. 254–259, Mar. 2007.
- [2] M. Grossman, C. McMillan, P. Moore, L. Ding, G. Glosser, M. Work, J. Gee, "What's in a name: Voxel-based morphometry

analysis of MRI and naming difficulty in Alzheimer's disease, frontotemporal dementia and corticobasal degeneration," *Brain*, vol. 127, no. 3, pp. 628–649, 2004.

[3] N.G.N.Prasad, G.Kranthi Kumar, G.Tirumala Vasu "A Hybrid Automated 3D Segmentation in Brain MRI" *IJECT Vol. 2, SP-1, Dec. 2011* *IJECT Vol. 2, SP-1, Dec. 2011*

[4] Hasan, Gholamreza Anbarjafari Discrete "Wavelet Transform-Based Satellite Image Resolution Enhancement" *IEEE TRANSACTIONS ON GEOSCIENCE AND REMOTE SENSING, VOL. 49, NO. 6, JUNE 2011*

[5] Albert Huang (S'05), Roger Tam, Rafeef Abugharbieh (M'03) "A Hybrid Geometric-Statistical Deformable Model for Automated 3-D Segmentation in Brain MRI" *IEEE TRANSACTIONS ON BIOMEDICAL ENGINEERING, VOL. 56, NO. 7, JULY 2009*

[6] Kinebuchi, D.D. Muresan, and T.W. Parks, "Image interpolation using wavelet based hidden Markov trees," in *Proc. IEEE ICASSP*, 2001, vol. 3, pp7–11

[7] Y. Piao, L. Shin, and H. W. Park, "Image resolution enhancement using inter-sub band correlation in wavelet domain," in *Proc. IEEE ICIP*, 2007, vol. 1, pp. I-445–I-448.

[8] D. W. Paty, D. Li, G. J. Zhao, "MRI in Multiple Sclerosis- Implications for Diagnosis and Treatment", 2nd ed. UBC MS/MRI Research Lab., Vancouver, BC, Canada, Rep. for Ares-Serono SA, 1999.

[9] H. Demirel, G. Anbarjafari, and S. Izadpanahi, "Improved motion-based localized super resolution technique using discrete wavelet transform for low resolution video enhancement," in *Proc. 17th EUSIPCO*, Edinburgh, U.K., Aug. 2009, pp. 1097–1101.

[10] T. Celik, C. Direkoglu, H. Ozkaramanli, H. Demirel, and M. Uyguroglu, "Region-based super-resolution aided facial feature extraction from lowresolution video sequences," in *Proc. IEEE ICASSP*, Philadelphia, PA, Mar. 2005, vol. II, pp. 789–792.

[11] H. Demirel and G. Anbarjafari, "Satellite image resolution enhancement using complex wavelet transform," *IEEE Geosci. Remote Sens. Lett.*, vol. 7, no. 1, pp. 123–126, Jan. 2010.

[12] L. Yi-bo, X. Hong, and Z. Sen-yue, "The wrinkle generation method for facial reconstruction based on extraction of partition wrinkle line features and fractal interpolation," in *Proc. 4th ICIG*, Aug. 22–24, 2007, pp. 933–937.

[13] Y. Rener, J. Wei, and C. Ken, "Downsample-based multiple description coding and post-processing of decoding," in *Proc. 27th CCC*, Jul. 16–18, 2008, pp. 253–256.

[14] C. B. Atkins, C. A. Bouman, and J. P. Allebach, "Optimal image scaling using pixel classification," in *Proc. ICIP*, Oct. 7–10, 2001, vol. 3, pp. 864–867.

B.Naresh Kumar received the B.Tech degree in Electronics and Communication Engineering in 2009 from the University college of Engineering, JNT University, Kakinada and pursuing M.Tech degree Instrumentation and Control Systems from JNT University, Kakinada. His areas of interest include Instrumentation, Control Systems, and MATLAB and communication systems.

[Mail to: bnk9933@gmail.com](mailto:bnk9933@gmail.com).

M.Sailaja received the Ph.D in electronics and Communication Engineering from the JNT University in 2009, persuade M.S. in U.S.A. She has been working at different companies and since 1994 working in University College of Engineering, JNTU Kakinada. [Mail to: sailaja.hece@gmail.com](mailto:sailaja.hece@gmail.com)

